Tumor cell plasticity in endometrioid carcinoma is regulated by neuronal membrane glycoprotein M6-b

SHINYA KUSUMOTO[1,2], JUN-ICHIRO IKEDA[3], MASAKO KURASHIGE[1], ETSUKO MAENO-FUJINAMI[1], SHINICHIRO TAHARA[1], TAKAHIRO MATSUI[1], SATOSHI NOJIMA[1], DAISUKE OKUZAKI[4-6] and EIICHI MORII[1]

[1]Department of Pathology, Osaka University Graduate School of Medicine, Suita, Osaka 565-0871, Japan; [2]Department of Obstetrics and Gynecology, David Geffen School of Medicine, University of California Los Angeles, Los Angeles, CA 90095, USA; [3]Department of Diagnostic Pathology, Chiba University Graduate School of Medicine, Chiba 260-8670; [4]Single Cell Genomics, Human Immunology, WPI Immunology Frontier Research Center, Osaka University; [5]Genome Information Research Center, Research Institute for Microbial Diseases, Osaka University; [6]Institute for Open and Transdisciplinary Research Initiatives, Osaka University, Suita, Osaka 565-0871, Japan

Abstract. Tumor cell plasticity and tumor heterogeneity are involved in therapy resistance. Cancer stem cells (CSCs) refer to tumor cells that have the ability to self-renew, and generate the diverse cells that comprise the tumor and complicate tumor heterogeneity. In recent years, CSCs have been reported to emerge from non-CSCs, which is known as tumor cell plasticity; however, the mechanism has not been fully elucidated. The present study investigated tumor cell plasticity from the viewpoint of aldehyde dehydrogenase 1 family member A1 (ALDH1A1) activity, which is one of the markers of CSCs. In the endometrioid carcinoma cell line HEC-1B, the ALDH1A1-low population spontaneously yielded an ALDH1A1-high population, mimicking tumor cell plasticity, and it was revealed that the mixture of the ALDH1A1-high population with the ALDH1A1-low population sometimes accelerated the transition from an ALDH1A1-low to ALDH1A1-high population. Two distinct HEC-1B sublines were established. One of the two sublines accelerated such a transition and the other did not show such acceleration. In the former subline, the effect of the ALDH1A1-high population was abolished when the direct cell-cell contact between ALDH1A1-high and ALDH1A1-low populations was inhibited. By comparing the two sublines, the neuronal membrane glycoprotein M6-b (GPM6B) was identified as the candidate mediating tumor cell plasticity. GPM6B was expressed in the border of ALDH1A1-expressing tumor cells and non-expressing tumor cells in clinical samples of EC. Notably, knockout of GPM6B decreased ALDH1A1 expression, whereas its overexpression increased the expression of ALDH1A1, suggesting that GPM6B mediated the induction of ALDH1A1 and the plasticity of CSCs.

Introduction

We reported previously that aldehyde dehydrogenase (ALDH)1A1, a potential marker of cancer stem cells (CSCs) (1,2), was related to tumorigenic potential in endometrioid carcinoma (EC) (3). CSCs refer to tumor cells that have the ability to self-renew and generate the diverse cells that comprise the tumor (4,5). Recent years, CSCs are reported to emerge from non-CSCs, called tumor cell plasticity (6,7), however, the mechanism has not been fully elucidated. In this study, we investigated the tumor cell plasticity from the viewpoint of ALDH1A1 activity.

In EC cell line HEC-1B, ALDH1A1-low population spontaneously yielded ALDH1A1-high population, mimicking tumor cell plasticity, and we found that the mixture of ALDH1A1-high population sometimes accelerated the transition from ALDH1A1-low to ALDH1A1-high population. We established two distinct HEC-1B sublines, in which ALDH1A1-high population accelerated such transition and ALDH1A1-high population did not show such acceleration. By comparing two sublines, we focused neuronal membrane glycoprotein M6-b (GPM6B) as the candidate mediating tumor cell plasticity.

GPM6B is a transmembrane protein that belongs to the proteolipid protein family. GPM6B is expressed in the central nervous system (8). GPM6B is related to the process of neuronal myelination, stabilizes the axonal membranes, and promotes neuronal differentiation (9-11). In the functional analysis of GPM6B in tumors, there is only a report that GPM6B has a cancer-suppressing effect in prostate cancer (12), and the function of GPM6B in EC is unknown.

Correspondence to: Professor Eiichi Morii, Department of Pathology, Osaka University Graduate School of Medicine, 2-2 Yamada-oka, Suita, Osaka 565-0871, Japan
E-mail: morii@molpath.med.osaka-u.ac.jp

Abbreviations: EC, endometrioid carcinoma; ALDH1A1, aldehyde dehydrogenase 1 family member A1; GPM6B, neuronal membrane glycoprotein M6-b

In this study, we investigated the tumor cell plasticity from the viewpoint of ALDH1A1 activity, and found that the tumor cell plasticity sometimes accelerated by direct contact between cancer cells. We focused on GPM6B as the candidate mediating tumor cell plasticity and started functional analysis of GPM6B. The knocked-out of GPM6B decreased and its overexpression increased the expression of ALDH1A1. Thus, it might be suggested that GPM6B mediated the induction of ALDH1A1 and the plasticity of CSCs.

Materials and methods

Patients. The study was approved by the Ethical Review Board of the Graduate School of Medicine, Osaka University (approval no. 15234), and was performed in accordance with the committee guidelines and regulations. We examined 47 patients undergoing surgery for EC at Osaka University Hospital from 2011 to 2014. All patients provided written informed consent. The clinicopathological features of the enrolled patients were shown in Table I. Resected specimens were fixed in 10% formalin and processed for paraffin embedding. Specimens were stored at room temperature in a dark room, sectioned at 4 μm thickness, and subjected to immunohistochemical analysis.

Cell lines and cell culture. The human EC cell lines HEC-1B and HEC108 were obtained from the Health Science Research Resources Bank of Osaka, Japan. Cell lines were cultured in Dulbecco's modified Eagle's medium (DMEM)-High glucose supplemented with 10% FBS, penicillin (100 IU/ml), and streptomycin (100 μg/ml) and maintained at 37˚C in 5% CO_2.

Antibodies and reagents. The antibodies against ALDH1A1 and β-actin were used as previously reported (13). The antibody against GPM6B (HPA002913, Sigma-Aldrich) was used for immunohistochemistry (dilution at 1:200). The antibody against GFP (#2956, Cell Signaling Technology) was used for immunoblotting (dilution at 1:500).

Plasmid. The plasmids Empty-EGFP (pRP-EGFP-CMV) and GPM6B [pRP-EGFP-CAG-FLAG/3xGGGGS/hGPM6B (NM_001001995.3)] were obtained from Vector Builder, Inc (Chicago, IL, USA).

Flow cytometry. The ALDEFLUOR kit (STEM CELL Technologies) was used according to the manufacturer's instructions. Cells were analyzed by FACS CantoII and AriaII flow cytometer (BD Biosciences, Franklin Lakes, NJ, USA). Data analysis was perfomed using Cell Quest software (BD Biosciences).

Immunofluorescence. The ALDEFLUOR kit and PKH26 Red Fluorescent Cell Linker Kit (SIGMA-ALDRICH) were used according to the manufacturer's protocols. Fluorescence signals were visualized using fluorescence microscope (BZ-8000, KEYENCE, Osaka, Japan).

Generation of subline cells using plasma-activated medium. For generation of HEC-1B subline cells, original cells were treated with threefold diluted plasma-activated medium (PAM) which was culture medium irradiated by non-thermal plasma device that containing of gas, electrons, ions, radicals, and ultraviolet light as previously described (14). PAM induced apoptosis in a large number of cells due to production of reactive oxygen species (ROS) such as H2O2. Therefore, we selected the single cell survived from ROS using microscope. After the selected cell was cultured in 96-well plate, cells proliferated in 6-well plate. The same procedure was repeated once more to prepare HEC-1B subline cells.

RNA sequencing analysis. Total RNA was extracted using the miRNeasy Mini Kit (Qiagen, Hilden, Germany) according to the manufacturer's instructions. cDNA libraries were constructed using the TruSeq Stranded mRNA Sample Prep Kit (Illumina, San Diego, CA, USA) according to the manufacturer's protocol. Sequencing was undertaken on the Illumina HiSeq 2500 platform in 75-base single-end mode. Casava version 1.8.2 software (Illumina) was used for base calling. The sequenced reads were mapped to a human reference genome sequence (hg19) using TopHat version 2.0.13 (http://ccb.jhu.edu/software/tophat/index.shtml), Bowtie2 version 2.2.3 (http://bowtie-bio.sourceforge.net/bowtie2/index.shtml), and SAMtools version 0.1.19 (http://samtools.sourceforge.net/). The fragments per kilobase of exon per million mapped fragments values were calculated using Cuffnorm version. 2.2.1 (http://cole-trapnell-lab.github.io/cufflinks/) to identify upregulated (2.0-fold, P<0.05) and downregulated (-0.5-fold, P<0.05) genes.

Generation of GPM6B-KO cell lines. GPM6B in HEC-1B was disrupted using the TrueGuide™ CRISPR/Cas9 system (Invitrogen, Carlsbad, CA, USA), in accordance with the manufacturer's instructions. The crRNA (A35509, CRISPR714997_CR, sequence: GUGUUGCUCAAGAAU CGCCA, target exon: exon2, Invitrogen) was annealed with TrueCut™ tracrRNA (Invitrogen). HEC-1B cells was co-transfected with the gRNA (crRNA:tracrRNA duplex) and TrueCut™ Cas9 Protein v2 (Invitrogen) using Lipofectamine™ CRISPRMAX™ Cas9 Transfection Reagent (Invitrogen). Single cell clones were then isolated by using limiting dilution cloning in 96-well plates. The positive clones were confirmed the absence of GPM6B by PCR of genomic sequence. Untransfected HEC-1B parent cells (WT) was used as a negative control.

Generation of HEC-1B and HEC108 cells expressing GPM6B-GFP. The plasmid Empty-GFP was transfected into HEC-1B and HEC108 cells using Lipofectamine 3000 reagent (Thermo Fisher Scientific). The plasmid GPM6B-GFP was transfected into HEC-1B (GPM6B-KO) and HEC108 cells. Green population was sorted with Cell Sorter SH800ZDP (SONY, Tokyo, Japan). When colonies formed after passage, we picked up different colonies and named OE1 and OE2. Untransfected HEC108 parent cells (WT) was used as a negative control. HEC1B and HEC-108 transfected with empty vector (EV) was used as another negative control.

Reverse transcription-quantitative PCR (RT-qPCR). The RT-qPCR was performed with StepOnePlus™ Real-Time PCR instrument (Applied Biosystems, Foster City, CA) using Taqman probe/primer sets specific for human GPM6B

Table I. Clinicopathological features of enrolled cases.

Characteristic	Number of cases
Histological grade	
Grade 1	24
Grade 2	16
Grade 3	7
Total	47
Clinical stage	
IA	26
IB	2
II	7
III	12
Total	47

(Hs01041077_m1). GAPDH was used as a reference for gene amplification (Applied Biosystems).

PCR. Cells were rinsed three times with PBS and lysed in 500 μl of lysis buffer [1xSSC (418 μl), 1M Tris-HCl (pH 7.5) (5 μl), 0.5M EDTA (pH 8.0) (1 μl), 10% SDS (50 μl), 20 mg/ml Proteinase K (FUJIFILM) (25 μl), 10 mg/ml RNase A (Invitrogen) (1 μl)]. The samples were mixed by vortexing and centrifugation at 15,310 g for 10 min at room temperature. After centrifugation at high speed, the upper phase was carefully removed and transferred to a new tube. A mixture of Phenol: Chloroform: Isoamyl Alcohol (Nacalai) was added in equal volumes to samples and the samples were mixed gently and the aqueous layer was transferred into a new tube. After ethanol precipitation, precipitated DNA was dissolved in 30 μl of sterile 1xTE buffer (pH 8.0). Extracted genomic DNA was amplified with KOD FX Neo (TOYOBO). The following primers which include protospacer adjacent motif were used to amplify DNA:

(Forward) 5'-CCGTGGCGATTCTTGAGCAAC-3'
(Reverse) 5'-ATGCCCTGGGATCTGCTCTTC-3'
The following primers were used to check the disrupted alleles:
Human GPM6B:
Exon 2:
(Forward) 5'-ACTGCTCTGCCATTCACTACCCTTCCAG-3'
(Reverse) 5'-ACGCACCACCACGCCCAGCTAAATTTTT-3'.

PCR was done on the T100 Thermal Cycler (Bio-Rad, USA). The PCR amplification consisted of an initial denaturation for 2 min at 94˚C, followed by 5 cycles of denaturation (10 sec, 98˚C) and extension (30 sec, 74˚C), 5 cycles of denaturation (10 sec, 98˚C) and extension (30 sec, 72˚C), 5 cycles of denaturation (10 sec, 98˚C) and extension (30 sec, 70˚C), 30 cycles of denaturation (10 sec, 98˚C) and extension (30 sec, 68˚C). The final extension step was carried out at 68˚C for 7 min. Its analyzing was performed using 1.5% agarose gel electrophoresis and visualized using gel documentation (AE-9000 E-Graph, ATTO, Japan).

Immunohistochemistry. Immunohistochemical staining was conducted by the Dako Autostainer Link 48 + (Dako/Agilent Technologies, Inc.) according to the manufacturer's instructions. Primary antibodies are incubated for 30 min at room temperature.

Immunoblotting. Studies were performed as previously reported (13). LAS-4000 Image Analyzer (GE Healthcare, Chicago, IL, USA) or ChemiDoc Touch (Bio-Rad) were used for the detection of antibody reaction. The expression of β-Actin was used as a loading control.

Statistical analysis. Statistical analyses were performed using JMP Pro 14 software (SAS Institute). *In vitro* experiments were performed at least two times. The data are presented as means ± standard error of the mean of independent experiments. The significance of the differences was determined using Mann Whitney U test. The log-rank test was used for survival analysis. Kaplan-Meier survival plots were made by using GraphPad Prism 9. $P<0.05$ was considered to indicate a statistically significant difference.

Results

Confirmation of plasticity of cancer cells. To validate the tumor cell plasticity, we conducted Aldefluor assay using EC cell line HEC-1B. After culturing ALDH1A1-low cells, the cell distribution was analyzed by the assay. ALDH1A1-low population spontaneously yielded ALDH1A1-high population (Fig. 1A). Next, we stained ALDH1A1-low cells red using the PKH26 Red Fluorescent Cell Linker Kit and conducted Aldefluor assay. The percentage of cells that turned yellow in the total cell number was defined as Plasticity index (Fig. 1B). Furthermore, we found that the mixture of ALDH1A1-high population sometimes accelerated the plasticity index and observed changes in tumor cells with low ALDH1A1 activity under a fluorescence microscope (Fig. 1C and D). Many color changes were observed in the adhesive areas between tumor cells (Fig. 1D).

Direct contact with cancer cells promotes tumor plasticity. We speculated that physical contact between cells contributed to the activation of ALDH1A1. First, we generate some sublines of HEC-1B cells using PAM and co-cultured ALDH1A1-high cells and ALDH1A1-low cells by a method of culturing two types of cells in the same dish and a method of culturing the two types of cells so that they do not contact with each other via transwell (Permeable Supports 3.0 μm Polycarbonate membrane, Corning) (Fig. 2A). In subline A, the former method had a higher plasticity index than the latter method, however, there was no difference in subline B (Fig. 2B). And then, we extracted RNAs of subline A and B. We compared the RNA expression of both cells and focused on GPM6B as the candidate mediating tumor cell plasticity (Fig. 2C; Tables II and SI). Next, we performed immunohistochemistry analysis of ALDH1A1 and GPM6B in clinical samples of EC tissues and found that GPM6B tended to express in the border of ALDH1A1 expressing tumor cells and non-expressing tumor cells (Fig. 2D).

GPM6B promotes ALDH1A1 expression in EC cell lines. To examine the significance of GPM6B in EC, we disrupted the
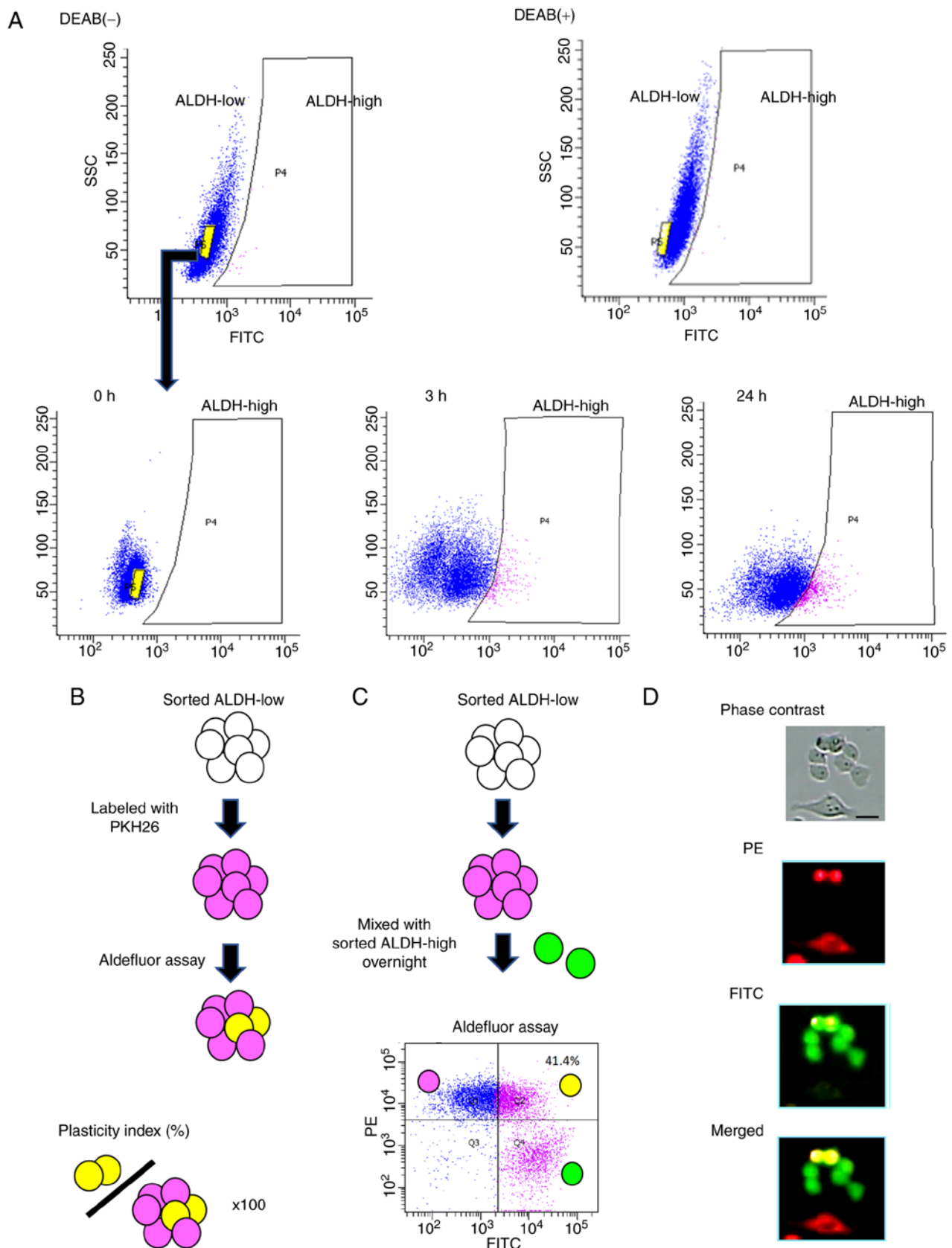
Figure 1. Confirmation of plasticity of cancer cells. (A) When the extracted cells with low ALDH1A1 activity were cultured for 0, 3 and 24 h, their ALDH1A1 activity increased. (B) A schematic of the plasticity index. (C) Schematic of co-culturing cells with ALDH1A1 high/low activity. (D) Representative images of immunofluorescence (PKH26 and anti-Aldefluor). Scale bars: 50 μm. ALDH1A1, aldehyde mehydrogenase 1 family member A1.

GPM6B gene in HEC-1B cells, using the CRISPR/Cas9 system and successfully established GPM6B-knockout (KO) HEC-1B cells (Fig. 3A and B). Furthermore, we showed the transfection efficiency (Fig. S1A), and we constructed HEC-1B cells
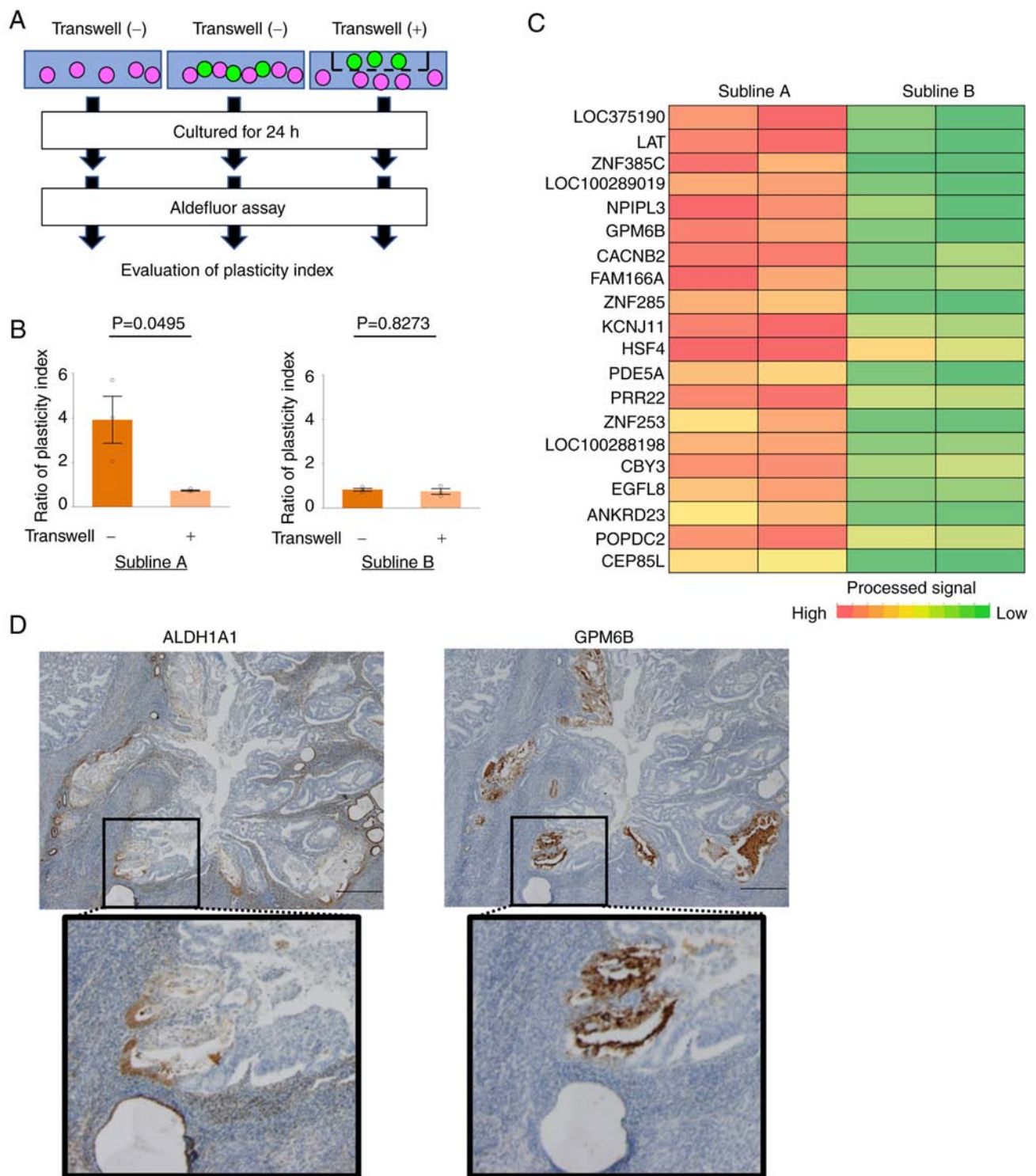
Figure 2. Direct contact with cancer cells promotes tumor plasticity. (A) Schematic of experimental approach for co-culturing cells with ALDH1A1 high/low activity. (B) Ratio of plasticity index of subline A and B. P-values were determined by the Mann Whitney U test. (C) Genes upregulated in subline A compared with subline B by RNA-seq. The fold change cut-off value was set to 2.0. (D) Representative image of immunohistochemistry of ALDH1A1 and GPM6B in endometrioid carcinoma tissue. Black scale bar, 500 μm. ALDH1A1, aldehyde dehydrogenase 1 family member A1; GPM6B, neuronal membrane glycoprotein M6-b.

(GPM6B-KO) stably expressing GPM6B (Figs. 3C and S1B). GPM6B knockout in HEC-1B cells resulted in a decreased level of ALDH1A1 expression and GPM6B expressing HEC-1B cells (GPM6B-KO) resulted in an increased level of ALDH1A1 (Fig. 3D and Table SII). Similarly, we constructed GPM6B-expressing HEC108 cells (OE1 and OE2)

(Figs. 3E and S1B). GPM6B expressing HEC108 cells resulted in an increased level of ALDH1A1 (Fig. 3F).

High GPM6B is related with poor prognosis. Due to a limited number of enrolled cases in this study, we examined the effect of high GPM6B on prognosis with three kinds of publicly

Table II. Top 20 genes upregulated in subline A.

Fold change	P-value	Gene symbol	Description
4.003	0.049	LOC375190	N/A
3.585	0.009	LAT	Linker for activation of T cells
3.399	0.023	ZNF385C	Zinc finger protein 385C
3.322	0.050	LOC100289019	Uncharacterized LOC100289019
3.268	0.039	NPIPL3	Nuclear pore complex interacting protein-like 3
3.091	0.019	GPM6B	Neuronal membrane glycoprotein M6B
2.856	0.012	CACNB2	Calcium channel, voltage-dependent, beta 2 subunit
2.665	0.040	FAM166A	Family with sequence similarity 166, member A
2.593	0.005	ZNF285	Zinc finger protein 285
2.589	0.008	KCNJ11	Potassium inwardly-rectifying channel, subfamily J, member 11
2.407	0.024	HSF4	Heat shock transcription factor 4
2.362	0.021	PDE5A	Phosphodiesterase 5A, cgmp-specific
2.285	0.005	PRR22	Proline rich 22
2.278	0.030	ZNF253	Zinc finger protein 253
2.240	0.004	LOC100288198	Uncharacterized LOC100288198
2.179	0.008	CBY3	Chibby homolog 3 (*Drosophila*)
2.171	0.015	EGFL8	EGF-like-domain, multiple 8
2.073	0.027	ANKRD23	Ankyrin repeat domain 23
2.067	0.013	POPDC2	Popeye domain containing 2
2.028	0.008	CEP85L	Centrosomal protein 85kda-like

available datasets; gene expression profiling interactive analysis (GEPIA)2, human protein atlas, and the cancer genome atlas (TCGA). In GEPIA2 of uterine corpus endometrial carcinoma, high GPM6B expression was marginally correlated with poor overall survival of the patients (Fig. 4A), in which group cutoff was set as quartile (http://gepia2.cancer-pku.cn/#survival). The data of human protein atlas revealed high GPM6B expression was correlated with poor overall survival of endometrial carcinoma (https://www.proteinatlas.org/ENSG00000046653-GPM6B/pathology/endometrial+cancer), in which 432 cases of GPM6B-high and 109 cases of GPM6B-low were enrolled and the best expression cut-off score 1.94 was applied (Fig. 4B). The median follow-up time of human protein atlas was 2.5 years and the p-value was 0.037. Lastly, we examined TCGA database, in which the enrolled endometrial carcinoma cases were divided into recently published classification (15); POLE type (ultramutated) (POLE), microsatellite instability (MSI), copy number low (CN-low), and copy number high (CN-high). Sixteen cases of POLE, 65 cases of MSI, 87 cases of CN-low and 58 cases of CN-high were examined in TCGA database. When cutoff was set as quartile, patients with high GPM6B expression had significantly shorter OS compared with those with low GPM6B expression in CN-high group but not in other groups (Fig. 4C).

Discussion

We identified a new function of GPM6B in EC cells. GPM6B contributed to the tumor cell plasticity in EC. We reported previously that a potential marker of CSCs; ALDH1A1 was related to tumorigenic potential in EC (3). The ALDH1A1-high cells are thought to be target for treatment. However, the tumor cell plasticity is reported to occur (6,7) and we should target the ALDH1A1-low cells which have a potential to become ALDH1A1-high cell.

To find the mechanism of the tumor cell plasticity, we focused on the direct contact between tumor cells. We collected some subclones from HEC-1B cells and tested the plasticity index according to Figs. 1C and 2A. We revealed that the biological ramification of direct cell-cell contact between tumor cells was one of triggers for the tumor cell plasticity. We extracted RNAs of cells with high/low plasticity index and compared the RNA expression of both cells. Among membrane proteins GPM6B was only high expression level in cells with high plasticity index.

GPM6B is less understood for cancer research and recently reported to work as a tumor suppressor in prostate cancer (12). To examine the significance of GPM6B in EC, we generated GPM6B-KO and GPM6B-expressing cells. We found that ALDH1A1 expression was regulated by GPM6B. Thus, we revealed another aspect of GPM6B for cancer. Notably, GPM6B was expressed in the border of ALDH1A1 expressing tumor cells and non-expressing tumor cells in clinical samples of EC. That is, GPM6B is not expressed in ALDH1A1 high expression area. GPM6B might be necessary for only increasing ALDH1A1. Further investigation is needed to uncover the mechanism.

In prognostic analysis, GPM6B was a prognostic factor. Though ALDH1A1 was a prognostic factor, the gene regulating tumor cell plasticity was also prognostic factor. It might be important to target not only CSCs but also non-CSCs which
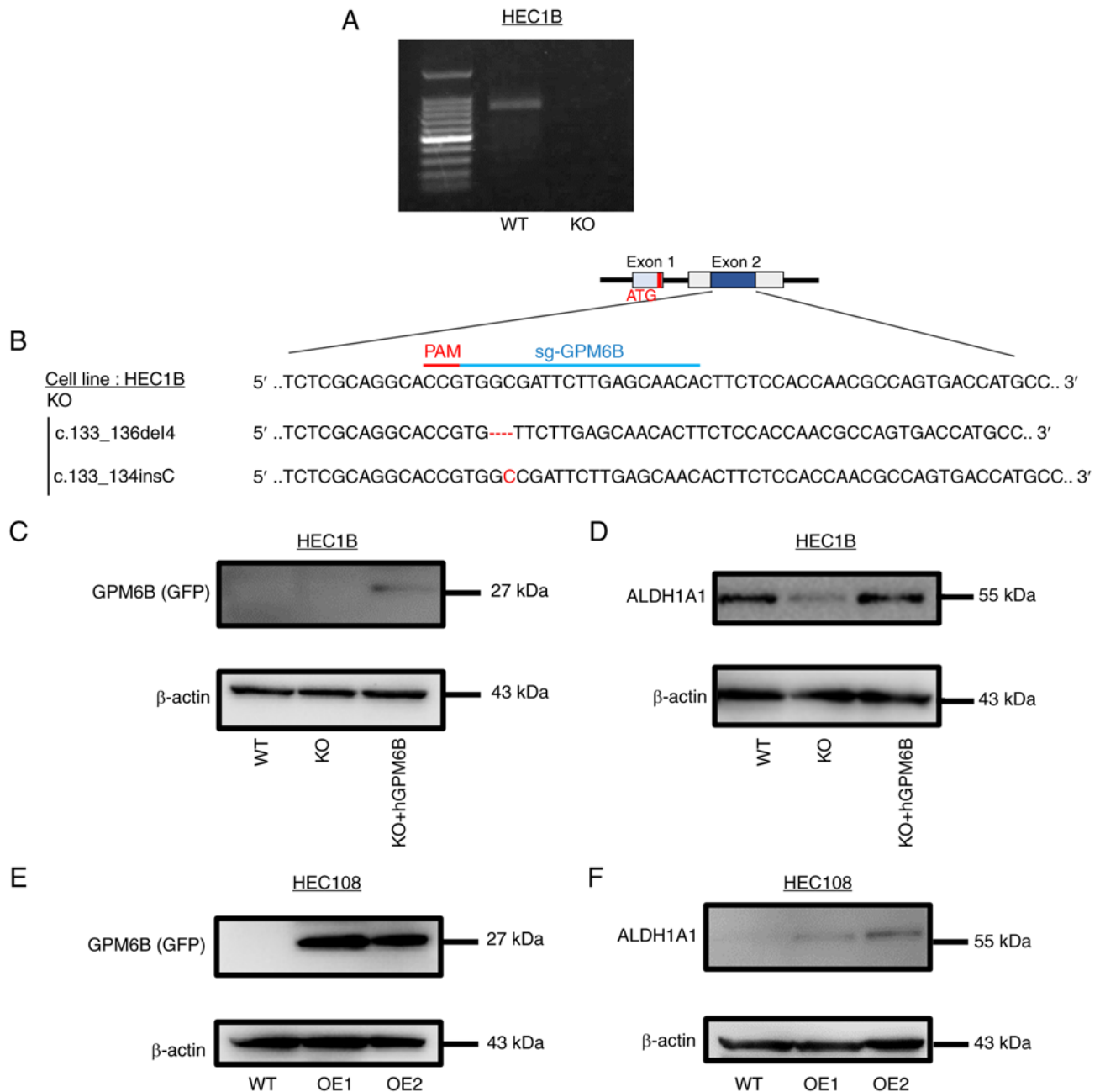
Figure 3. GPM6B promotes ALDH1A1 expression in EC cell lines. (A) PCR of GPM6B in parent cells (WT) and GPM6B-KO HEC-1B cells. (B) A schematic of the single-guide (sg) RNA-targeting sites in the human GPM6B gene. The guide sequence of the human GPM6B gene was targeting exon 2 and it was 5'-TGGCGATTCTTGAGCAACAC-3. Targeting site and protospacer adjacent motif (PAM) are indicated as red-colored bar. Sequence alignments of the wild-type GPM6B gene and the disrupted alleles from GPM6B-KO clone are shown. Deleted regions are indicated with red-colored dashes and insertion parts are shown in red. (C) Immunoblotting of GPM6B(GFP) in WT, GPM6B-KO and GPM6B-KO + hGPM6B HEC-1B cells. (D) Immunoblotting of ALDH1A1 in HEC-1B cells (WT, KO, KO + hGPM6B) (E) Immunoblotting of GPM6B in WT, GPM6B-OE1 and GPM6B-OE2 HEC108 cells. (F) Immunoblotting of ALDH1A1 in HEC108 cells (WT, GPM6B-OE1, GPM6B-OE2). ALDH1A1, aldehyde dehydrogenase 1 family member A1; GPM6B, neuronal membrane glycoprotein M6-b; KO, knockout; OE, overexpressing; WT, wild type.

have a potential to become CSCs for cure EC. Moreover, high GPM6B expression may be more effective as prognostic factor when the EC cases are classified to CN-high. CN-high is a worse prognostic classification as compared to POLE, MSI and CN-low. Factors enhancing plasticity of non-CSCs to CSCs might play important roles in prognosis.

In summary, direct cell-cell contact between tumor cells influenced on the tumor cell plasticity. GPM6B regulated ALDH1A1 expression. Furthermore, GPM6B was also a prognostic factor. These results suggest that GPM6B mediated the induction of ALDH1A1 and we have to consider tumor cell plasticity to cure EC.
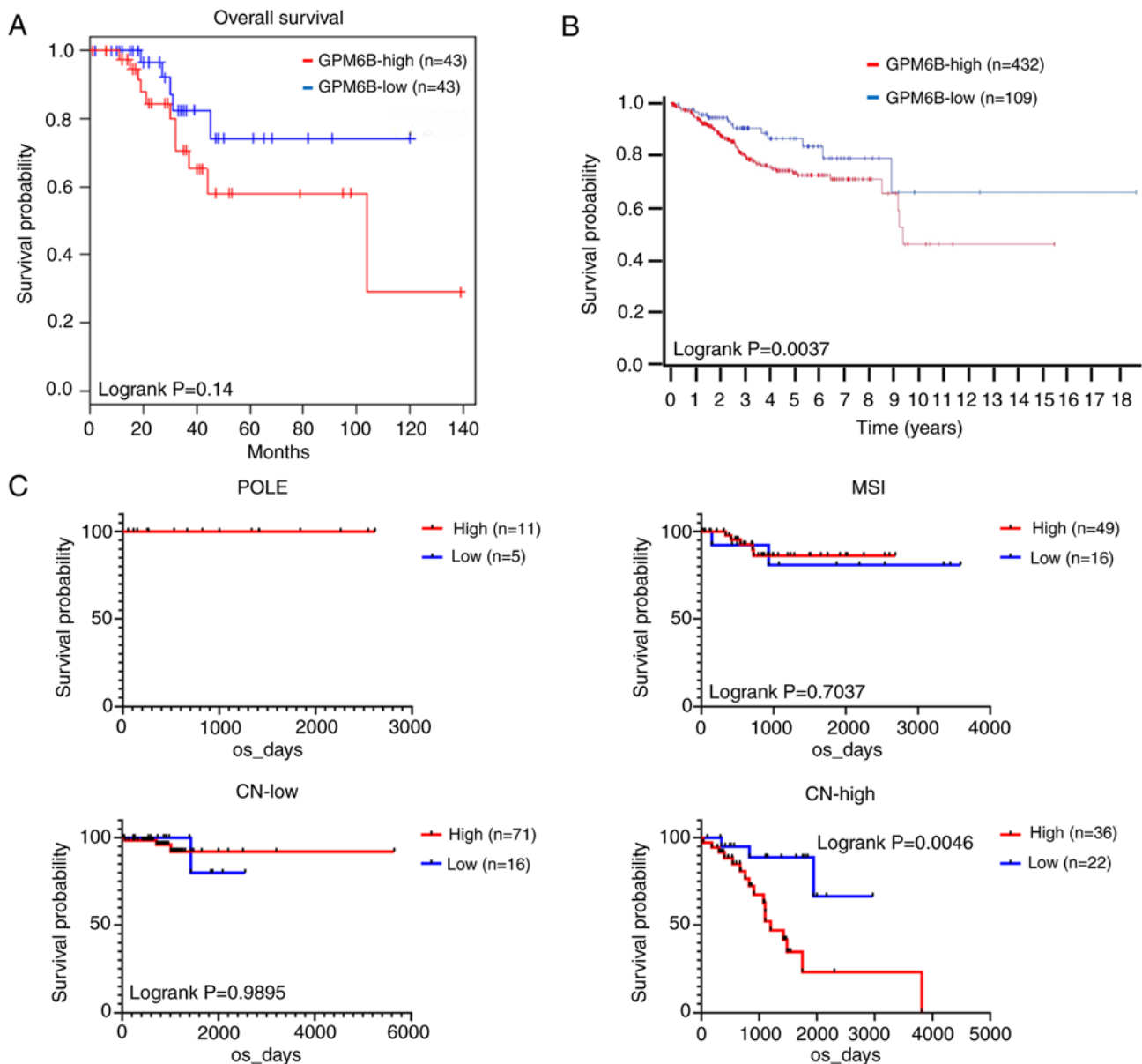
Figure 4. High GPM6B is related with poor prognosis. (A) Kaplan-Meier plots for GPM6B expression in endometrial carcinoma derived from the GEPIA2 dataset (http://gepia2.cancer-pku.cn/#index). (B) Kaplan-Meier plots for GPM6B expression in endometrial carcinoma derived from the human protein atlas dataset (https://www.proteinatlas.org/ENSG00000046653-GPM6B/pathology/endometrial+cancer). (C) Kaplan-Meier survival plots of POLE, MSI, CN-high, and CN-low cases of TCGA database. GPM6B, neuronal membrane glycoprotein M6-b; POLE, POLE type (ultramutated); MSI, microsatellite instability; CN, copy number.

Authors' contributions

SK, JII and EM were involved with conception and design. SK, JII, DO and EM analyzed and interpreted the data. SK, JII, EMF, MK, ST, TM, SN and EM performed experiments and analyzed data. SK, JII and EM wrote the manuscript. SK and EM confirm the authenticity of all the raw data. All authors read and approved the final manuscript, and are accountable for all aspects of the work.

Ethics approval and consent to participate

The study was approved by the Ethical Review Board of the Graduate School of Medicine, Osaka University (grant no. 15234), and was performed in accordance with the

committee guidelines and regulations. All patients provided written informed consent to participate in the study.

Patient consent for publication

Patient consent for publication was covered by the informed consent document.

Competing interests

The authors declare that they have no competing interests.

References

1. Ginestier C, Hur MH, Charafe-Jauffret E, Monville F, Dutcher J, Brown M, Jacquemier J, Viens P, Kleer CG, Liu S, *et al*: ALDH1 is a marker of normal and malignant human mammary stem cells and a predictor of poor clinical outcome. Cell Stem Cell 1: 555-567, 2007.
2. Jiang F, Qiu Q, Khanna A, Todd NW, Deepak J, Xing L, Wang H, Liu Z, Su Y, Stass SA and Katz RL: Aldehyde dehydrogenase 1 is a tumor stem cell-associated marker in lung cancer. Mol Cancer Res 7: 330-338, 2009.
3. Rahadiani N, Ikeda J, Mamat S, Matsuzaki S, Ueda Y, Umehara R, Tian T, Wang Y, Enomoto T, Kimura T, *et al*: Expression of aldehyde dehydrogenase 1 (ALDH1) in endometrioid adenocarcinoma and its clinical implications. Cancer Sci 102: 903-908, 2011.
4. Hanahan D and Weinberg RA: Hallmarks of cancer: The next generation. Cell 144: 646-674, 2011.
5. Visvader JE and Lindeman GJ: Cancer stem cells in solid tumours: Accumulating evidence and unresolved questions. Nat Rev Cancer 8: 755-768, 2008.
6. Merrell AJ and Stanger BZ: Adult cell plasticity in vivo: De-differentiation and transdifferentiation are back in style. Nat Rev Mol Cell Biol 17: 413-425, 2016.
7. Yuan S, Norgard RJ and Stanger BZ: Cellular plasticity in cancer. Cancer Discov 9: 837-851, 2019.
8. Yan Y, Narayanan V and Lagenaur C: Expression of members of the proteolipid protein gene family in the developing murine central nervous system. J Comp Neurol 370: 465-478, 1996.
9. Bang ML, Vainshtein A, Yang HJ, Eshed-Eisenbach Y, Devaux J, Werner HB and Peles E: Glial M6B stabilizes the axonal membrane at peripheral nodes of Ranvier. Glia 66: 801-812, 2018.
10. Mita S, de Monasterio-Schrader P, Fünfschilling U, Kawasaki T, Mizuno H, Iwasato T, Nave KA, Werner HB and Hirata T: Transcallosal projections require glycoprotein M6-dependent neurite growth and guidance. Cereb Cortex 25: 4111-4125, 2015.
11. Werner HB, Krämer-Albers EM, Strenzke N, Saher G, Tenzer S, Ohno-Iwashita Y, De Monasterio-Schrader P, Möbius W, Moser T, Griffiths IR and Nave KA: A critical role for the cholesterol-associated proteolipids PLP and M6B in myelination of the central nervous system. Glia 61: 567-586, 2013.
12. He S, Huang Z, Li X, Ding Y, Sheng H, Liu B and Jia Z: GPM6B inhibit PCa proliferation by blocking prostate cancer cell serotonin absorptive capacity. Dis Markers 2020: 8810756, 2020.
13. Kusumoto S, Kurashige M, Ohshima K, Tahara S, Matsui T, Nojima S, Hattori S and Morii E: An immature inhibin-α-expressing subpopulation of ovarian clear cell carcinoma cells is related to an unfavorable prognosis. Cancer Med 10: 1485-1500, 2021.
14. Ikeda JI, Tanaka H, Ishikawa K, Sakakita H, Ikehara Y and Hori M: Plasma-activated medium (PAM) kills human cancer-initiating cells. Pathol Int 68: 23-30, 2018.
15. Kandoth C, Schultz N, Cherniack AD, Akbani R, Liu Y, Shen H, Robertson AG, Pashtan I, Shen R, Benz CC, *et al*: Integrated genomic characterization of endometrial carcinoma. Nature 497: 67-73, 2013.